

AdaptiveFL: Adaptive Heterogeneous Federated Learning for Resource-Constrained AIoT Systems

Chentao Jia
East China Normal University
Shanghai, China

Ming Hu*
Nanyang Technological University
Singapore, Singapore
hu.ming.work@gmail.com

Zekai Chen
East China Normal University
Shanghai, China

Yanxin Yang
East China Normal University
Shanghai, China

Xiaofei Xie
Singapore Management University
Singapore, Singapore

Yang Liu
Nanyang Technological University
Singapore, Singapore

Mingsong Chen*
East China Normal University
Shanghai, China
mschen@sei.ecnu.edu.cn

Abstract

Although Federated Learning (FL) is promising to enable collaborative learning among Artificial Intelligence of Things (AIoT) devices, it suffers from the problem of low classification performance due to various heterogeneity factors (e.g., computing capacity, memory size) of devices and uncertain operating environments. To address these issues, this paper introduces an effective FL approach named *AdaptiveFL* based on a novel fine-grained width-wise model pruning mechanism, which can generate various heterogeneous local models for heterogeneous AIoT devices. By using our proposed reinforcement learning-based device selection strategy, AdaptiveFL can adaptively dispatch suitable heterogeneous models to corresponding AIoT devices based on their available resources for local training. Experimental results show that, compared to state-of-the-art methods, AdaptiveFL can achieve up to 8.94% inference improvements for both IID and non-IID scenarios.

ACM Reference Format:

Chentao Jia, Ming Hu, Zekai Chen, Yanxin Yang, Xiaofei Xie, Yang Liu, and Mingsong Chen. 2024. AdaptiveFL: Adaptive Heterogeneous Federated Learning for Resource-Constrained AIoT Systems. In *61st ACM/IEEE Design Automation Conference (DAC '24)*, June 23–27, 2024, San Francisco, CA, USA. ACM, New York, NY, USA, 7 pages. <https://doi.org/10.1145/3649329.3655917>

1 Introduction

Although Federated Learning (FL) [1] has been increasingly studied in Artificial Intelligence of Things (AIoT) design [2–4] to enable knowledge sharing without compromising data privacy among devices, it suffers from the problems of large-scale deployment and low inference accuracy. This is mainly because most existing FL methods assume that the models on device are homogeneous.

*Corresponding authors

Permission to make digital or hard copies of all or part of this work for personal or classroom use is granted without fee provided that copies are not made or distributed for profit or commercial advantage and that copies bear this notice and the full citation on the first page. Copyrights for components of this work owned by others than the author(s) must be honored. Abstracting with credit is permitted. To copy otherwise, or republish, to post on servers or to redistribute to lists, requires prior specific permission and/or a fee. Request permissions from permissions@acm.org.

DAC '24, June 23–27, 2024, San Francisco, CA, USA

© 2024 Copyright held by the owner/author(s). Publication rights licensed to ACM.

ACM ISBN 979-8-4007-0601-1/24/06

<https://doi.org/10.1145/3649329.3655917>

When dealing with an AIoT system involving devices with various heterogeneous hardware resource constraints (e.g., computing capability, memory size), the overall inference performance of existing FL approaches is often greatly limited, especially when the data on devices are non-IID (Independent and Identically Distributed). To address this problem, various heterogeneous FL methods [5–9] have been proposed, which can be classified into two categories, i.e., *completely heterogeneous* and *partially heterogeneous* methods. The completely heterogeneous approaches [8, 9] rely on both device models with different structures for local training and knowledge distillation technologies to facilitate knowledge sharing among these models. As an alternative, the partially heterogeneous methods [5–7] adopt hypernetworks as full global models, which can be used to generate various heterogeneous device models to enable model aggregation based on specific model pruning mechanisms.

Although the state-of-the-art heterogeneous FL methods can improve the overall inference performance of devices, most of them cannot be directly applied to AIoT systems. As an example of completely heterogeneous FL, the need for extra high-quality datasets may violate the data privacy requirement. Meanwhile, due to the Cannikin Law, the learning capabilities of completely heterogeneous FL methods are determined by small models, which are usually hosted by weak devices with fewer data samples. Similarly, for partially heterogeneous FL methods, the coarse-grained pruning on hypernetworks may weaken the learning capabilities of the model. Things become even worse when such FL-based AIoT systems are deployed in uncertain environments [10] with dynamically changing available resources, since the assignment of improperly pruned models to devices will inevitably result in insufficient learning of local models, thus hampering the overall inference capability of AIoT systems. *Therefore, how to wisely and adaptively assign properly pruned heterogeneous models to devices in order to maximize the overall inference performance of all the involved heterogeneous models in resource-constrained scenarios is becoming a major challenge in FL-based AIoT systems.*

Intuitively, to alleviate the insufficient training of local models, heterogeneous models should share more key generalized parameters. For a Deep Neural Network (DNN), the number of parameters of shallow layers is typically smaller than those of deep layers. According to the observation in [11], pruning shallow layers rather than deep layers can result in greater performance degradation. In

other words, if the pruning happens at deep layers of DNN, the inference performance degradation of DNN is negligible, while the size of the models can be significantly reduced. Inspired by this fact, this paper presents an effective heterogeneous FL approach named AdaptiveFL, which uses a novel fine-grained width-wise model pruning mechanism to generate heterogeneous models for local training. In AdaptiveFL, devices can adaptively prune received models to accommodate their available resources. Since AdaptiveFL does not prune any entire layer, the pruned models can be trained directly on devices without additional parameters or adapters. To avoid exposing device status to the cloud server, AdaptiveFL adopts a Reinforcement Learning (RL)-based device selection strategy, which can select the most suitable devices to train models with specific sizes based on the historical size information of trained models. In this way, the communication waste caused by dispatching mismatched models can be drastically reduced. This paper makes the following three major contributions:

- We propose a fine-grained width-wise pruning mechanism to wisely and adaptively generate heterogeneous models in resource-constrained scenarios.
- We present a novel RL-based device selection strategy to select devices with suitable hardware resources for the given heterogeneous models, which can reduce the communication waste caused by dispatching mismatched large models.
- We perform extensive simulation and real test-bed experiments to evaluate the performance of AdaptiveFL.

2 Background and Related Work

Preliminaries to FL. Generally, an FL system consists of one cloud server and multiple dispersed clients. In each round, the cloud server will first send the global model to selected devices. After receiving the model, the devices conduct local training and upload the parameters of the model to the cloud server. Finally, the cloud server aggregates the received parameters to update the original global model. So far, almost all FL methods aggregate local models based on FedAvg[1] defined as follows:

$$\min_w F(w) = \frac{1}{K} \sum_{k=1}^K f_k(w), \text{ s.t., } f_k(w) = \frac{1}{|d_k|} \sum_{i=1}^{|d_k|} \ell(w, \langle x_i, y_i \rangle),$$

where K is the total number of clients, $|d_k|$ is the number of data samples hosted by the k^{th} client, ℓ denotes loss function (e.g., cross-entropy loss), x_i denotes a sample, and y_i is the label of x_i .

Model Heterogeneous FL. Model heterogeneous FL has a natural advantage in solving the problem of system heterogeneity, where submodels of different sizes can better fit heterogeneous clients. Relevant prior work includes studies of width-wise pruning, depth-wise pruning, and two-dimensional scaling. For width-wise pruning, Diao *et al.* [5] proposed HeteroFL, which prunes model architectures for clients with variant widths and conducted parameter-averaging over heterogeneous models. For depth-wise pruning, Kim *et al.* [6] proposed DepthFL, which obtains local models of different depths by pruning the deepest layers of the global model. Recently, Ilhan *et al.* [7] proposed a two-dimensional pruning approach called ScaleFL, which utilizes self-distillation to transfer the knowledge among submodels. However, existing approaches seldom consider the resource uncertainties associated with devices in real-world environments. Most of them employ a

coarse-grained way for model pruning. In addition, resource information is the key to dispatch the appropriate model for each client in their approach, yet in practical applications, obtaining accurate resource information for devices can be difficult.

To the best of our knowledge, AdaptiveFL is the first resource-adaptive FL framework for heterogeneous AIoT devices without collecting their resource information. Since AdaptiveFL adopts a fine-grained width-wise model pruning mechanism together with our proposed RL-based device selection strategy, it can be easily integrated into large-scale AIoT systems to maximize knowledge sharing among devices.

3 Our Approach

Figure 1 presents the framework and workflow of AdaptiveFL. As shown in the figure, the cloud server performs three key stages, i.e., model pruning, RL-based device selection, and model aggregation. In the model pruning stage, the cloud server prunes the entire global model into multiple heterogeneous models, which will be dispatched to devices for local training. In the RL-based device selection stage, the cloud server selects a best-fit device for each heterogeneous model based on the curiosity table and the resource table. In the model aggregation stage, the cloud server aggregates the weights of uploaded models and updates the global model.

In specific, each FL training round of AdaptiveFL includes six key steps as follows:

- **Step 1: Model Pruning.** The cloud server generates multiple heterogeneous models based on the full global model by using the *fine-grained width-wise model pruning* mechanism and stores the generated models to the model pool;
- **Step 2: Model Selection.** The cloud server randomly selects a list of generated heterogeneous models from the model pool as dispatched models for local training;
- **Step 3: Client Selection.** The cloud server selects a client for each dispatching model by using our RL-based selection strategy and dispatches the model to its selected client;
- **Step 4: Local Training.** AIoT devices adaptively prune the received model according to their local available resources and train the model on their local raw data;
- **Step 5: Model Uploading.** Devices upload the trained model to the cloud server;
- **Step 6: Model Aggregation.** The cloud server generates a new global model by aggregating the corresponding parameters of all the uploaded models.

3.1 Implementation of AdaptiveFL

Algorithm 1 details the implementation of AdaptiveFL. Before FL training, Lines 1-2 initialize the curiosity table T_c and the resource table T_r . Lines 3-29 present the details of FL training for each round. Line 4 splits the global model M into submodels in different size levels (i.e., small, medium and large) and stores them in model pool $R = \{m_{S_p}, m_{S_{p-1}}, \dots, m_{M_2}, m_{M_1}, m_{L_1}\}$, where hyperparameters p is the number of submodels in each level except L level, and it should be noted that the large model m_{L_1} is unpruned which is equivalent to the global model. Lines 6-27 present the FL training process of the models waiting for training, where the loop “for” is parallel. In Line 7, the function *RandomSel(.)* is to randomly select a model m_i from the model pool R . In Line 8, the function *ClientSel(.)* is to select a suitable client c_i for model m_i from client set C based

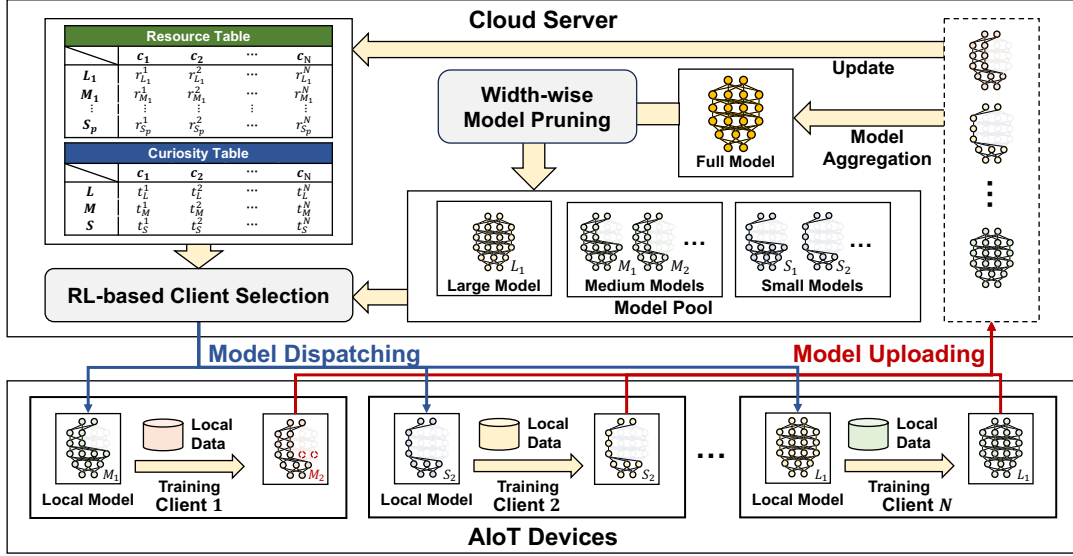


Figure 1. Framework and workflow of AdaptiveFL.

on RL-table T_c and T_r . In Line 9, the function $LocalTrain(\cdot)$ is to dispatch the model m_i to the selected client c_i for local training, and return the trained model m'_i with the local data size $|d_{c_i}|$ back to the server. Line 10 stores m'_i and $|d_{c_i}|$ to array ML_{back} and array Len , respectively, which are used for aggregation later. In addition, Lines 12-13 and Lines 14-26 present the updating process of T_c and T_r , respectively. In Lines 12-13, we updated the selection times for the level of the send and back models in T_c , respectively, where $type(m_i)$ means the level of model m_i , e.g., $type(m_{S_p})$ return the size level S . As for the update of T_r , we consider the following two cases: i) In Lines 15-18, since no pruning is done locally at the client c_i , which means that the resource capacity $\Gamma_{c_i} \geq size(m_i = m'_i)$, so we perform an increment operation for the training score in the table whose model size is larger than m_i ; ii) In Lines 20-25, it shows that $size(m'_i) \leq \Gamma_{c_i} \leq size(\hat{m}'_i)$, \hat{m}'_i here is the nearest greater model with m'_i in R . Thus, we use a penalty term τ to reduce the training score of the heterogenous model that is larger than \hat{m}'_i , while increasing the training score of the model m'_i .

3.2 Fine-Grained Width-Wise Model Pruning Mechanism

To enable devices to prune models according to their available resources adaptively, we adopt a width-wise pruning mechanism where the pruned model can be trained directly without additional adapters or parameters. Inspired by the observations in [11], we prefer to prune the parameters of deep layers, which enables large models trained by insufficient data to achieve higher performance. Specifically, our fine-grained width-wise model pruning mechanism is controlled by two hyperparameters, i.e., the width pruning ratio r_w and the index of the starting pruning layer I , respectively, where adjusting r_w can significantly change the model size while adjusting I can fine-tune the model size.

Width-Wise Model Pruning (r_w). To generate multiple models of different sizes, the cloud server prunes partial kernels in each layer of the model, where the number of kernels pruned is determined by the width pruning ratio $r_w \in (0, 1]$. Specifically, we

assume that W_g is the parameter of the global model M_g , d_k and n_k denote the output and input channel size of the k^{th} hidden layer of M_g , respectively. Then the parameters of the k^{th} hidden layer can be denoted as $W_g^k \in \mathbb{R}^{d_k \times n_k}$. With a width-wise pruning ratio r_w , the pruned weights of the k^{th} hidden layer can be presented as $W_{r_w}^k = W_g^k[:d_k \times r_w][:n_k \times r_w]$.

Layer-Wise Model Adjustment (I). To address performance fluctuations caused by uncertainty, our pruning mechanism supports fine-tuning the model size by adjusting the index of the starting pruning layer I . Note that to ensure that heterogeneous models share shallow layers, the index of the starting pruning layer must be set larger than the specific threshold τ . Specifically, assume that $I \geq \tau$, the weights of the k^{th} layer can be presented as $W_{r_w}^k = W_g^k[:d_k][:n_k]$ when $k \leq I$, and which can be presented as $W_{r_w}^k = W_g^k[:d_k \times r_w][:n_k \times r_w]$ when $k > I$.

Available Resource-Aware Pruning. To prevent failed training caused by limited resources, our pruning mechanism supports each device in pruning the received model adaptively according to its available resources. Specifically, assume that the available resource capacity of the device is Γ , the weight of the received model is W and $I \geq \tau$, and the width-wise pruning ratio r_w and the index of the starting pruning layer I can be determined as follows:

$$\arg \max_{r_w, I} size(prune(W; r_w, I)),$$

$$s.t., size(prune(W; r_w, I)) \leq \Gamma \text{ and } I \geq \tau,$$

3.3 RL-based Client Selection

Due to uncertainty and privacy concerns, the cloud server cannot obtain available resource information for AIoT devices. To avoid communication waste caused by dispatching unsuitable models, we propose an RL-based device selection strategy. By utilizing the information of historical dispatching and the corresponding received model $\langle m_i, m'_i \rangle$ of clients, RL can learn the information about the available resources of each device. Based on the learned

Algorithm 1: Implementation of AdaptiveFL

Input: i) T , training rounds; ii) C , client set; iii) K , the number of clients selected each round; iv) p , the number of model in each level.

```

1  $T_c[i][j] \leftarrow 1$  for  $i \in [1, 3], j \in [1, |C|]$ 
2  $T_r[i][j] \leftarrow 1$  for  $i \in [1, 2p + 1], j \in [1, |C|]$ 
3 for epoch  $E = 1, \dots, T$  do
4    $R = \{m_{S_p}, m_{S_{p-1}}, \dots, m_{M_2}, m_{M_1}, m_{L_1}\} \leftarrow \text{Split}(M)$ 
5   /*parallel for*/
6   for  $i = 1, \dots, K$  do
7      $m_i \leftarrow \text{RandomSel}(R)$ 
8      $c_i \leftarrow \text{ClientSel}(m_i, T_c, T_r, C)$  //RL-based Client Selection
9      $(m'_i, |d_{c_i}|) \leftarrow \text{LocalTrain}(c_i, m_i)$  // Local Training
10     $ML_{back}[i] \leftarrow m'_i, Len[i] \leftarrow |d_{c_i}|$ 
11    /* Update RL Table */
12     $T_c[\text{type}(m_i)][c_i] \leftarrow T_c[\text{type}(m_i)][c_i] + 1$ 
13     $T_c[\text{type}(m'_i)][c_i] \leftarrow T_c[\text{type}(m'_i)][c_i] + 1$ 
14    if  $m_i = m'_i$  then
15      for  $t = m_i, \dots, m_{L_1}$  do
16         $T_r[t][c_i] \leftarrow T_r[t][c_i] + 1$ 
17      end
18       $T_r[m_{L_1}][c_i] \leftarrow T_r[m_{L_1}][c_i] + p - 1$ 
19    else
20       $T_r[m'_i][c_i] \leftarrow T_r[m'_i][c_i] + p$ 
21       $\tau \leftarrow 0$ 
22      for  $t = m'_i, \dots, m_{L_1}$  do
23         $T_r[t][c_i] \leftarrow \max(T_r[t][c_i] - \tau, 0)$ 
24         $\tau \leftarrow \tau + 1$ 
25      end
26    end
27  end
28   $M \leftarrow \text{Aggregate}(m_{L_1}, ML_{back}, Len)$ 
29 end

```

information, RL can learn a strategy to select suitable devices for each heterogeneous model wisely.

Problem Definition. In our approach, the client selection process can be regarded as a Markov Decision Process [12], which can be presented as a four-tuple $MDP = \langle \mathcal{S}, \mathcal{A}, \mathcal{F}, \mathcal{R} \rangle$ as follows:

- \mathcal{S} is a set of states. We use a vector $s_t = \langle D_t, S, C_t, T_c, T_r \rangle$ to denote the state of AdaptiveFL, where D_t denotes the set of submodels that wait for dispatching, S is the list of the size information of all submodels in the model pool, C_t indicates the set of clients involved, T_c and T_r are the curiosity table and the resource table, respectively.
- \mathcal{A} is a set of actions. At the state of $s_t = \langle D_t, S, C_t, T_c, T_r \rangle$, the action a_t aims to select a suitable client $c_i \in C_t$ for the candidate model $m_i \in D_t$.
- \mathcal{F} is a set of transitions. It records the transition $s_t \xrightarrow{a_t} s_{t+1}$ with the action a_t .
- \mathcal{R} is the reward function. We combine the values in the resource table T_r and the curiosity table T_c of each client as the reward to guide the selection on this round.

Resource- and Curiosity-Driven Client Selection. Since there is an implicit connection between the model size with the resource budget, the model returned by the client can be used to determine the available resource range of the device. Specifically, AdaptiveFL uses a client resource table T_r to record the historical training score for each heterogeneous model on each client, where a higher score indicates that the client has a higher success rate in training the corresponding model. The resource reward for client c on submodel m_i is measured as follows:

$$R_s(m_i, c) = \frac{\sum_{k=T_p, T=\text{type}(m_i), k \in R}^{\sum_{t=k}^{L_1} T_r[m_t][c]}}{p \times \sum_{k=S_p, k \in R}^{L_1} T_r[m_k][c]}.$$

To balance the training times of the same model level on different clients, we utilize curiosity-driven exploration [4, 13] as one of the reward evaluation strategies, while the client who is selected fewer times on a size level of the model will get higher curiosity rewards. AdaptiveFL uses the curiosity table T_c to record the selection times of each client on a type of model, and performs Model-based Interval Estimation with Exploration Bonuses (MBIE-EB) [14] to calculate the curiosity reward as follows:

$$R_c(m_i, c) = \frac{1}{\sqrt{T_c[\text{type}(m_i)][c]}},$$

where $T_c[\text{type}(m_i)][c]$ indicates the total selection number of model type $\text{type}(m_i)$ on client c . To avoid the higher success rate of the large client leading to the lower probability of other clients being selected, we set the upper success rate of 50%, and the selection of clients whose success rate is beyond 50% will be determined by the curiosity reward. Consequently, the final reward for each client on the model m_i is calculated by combining resource reward R_s and curiosity reward R_c as follows:

$$R(m_i, c) = \min(0.5, R_s(m_i, c)) \times R_c(m_i, c).$$

In conclusion, based on the final reward, the probability that the client c is selected for model m_i is:

$$P(m_i, c) = \frac{R(m_i, c)}{\sum_{j=1}^{|C|} R(m_i, j)}.$$

3.4 Heterogenous Model Aggregation.

In our model pruning mechanism, since all the submodels are pruned based on the same full global model, the cloud server can update the global model by aggregating all the received heterogenous submodels according to the corresponding index of their parameters in the full model. Algorithm 2 details the aggregation process of our approach. Line 1 is the initialization of the process. Lines 2-17 update the parameters of each layer in the model. Line 3 initializes the variable L_w , which is used to count the total number of the training data size for each parameter. In Lines 4-8, the model parameters of each client are added with weights, which is the size of local data. For each client, the uploaded model often lacks some parameters compared to the complete model. Lines 10-16 take the average of the updated parameters. Note that if some parameters are not included in any uploaded model, they will keep their original values unchanged, which is shown in Line 14.

Algorithm 2: Heterogenous Model Aggregation

Input: i) $\theta = \{l_1^\theta, \dots, l_N^\theta\}$, global model weights; ii) $\{\theta_c\}_{c \in S}$, set of local model weights; iii) $\{|d_c|\}_{c \in S}$, set of local data size

Output: θ' , aggregated global model weights

```

1  $\theta' \leftarrow \text{Zero}(\theta)$ 
2 for  $k$  in  $1, \dots, N$  do
3    $L_w \leftarrow \text{Zero}(\text{len}(l_k^{\theta'}))$ 
4   for  $c$  in  $S$  do
5     for  $i$  in  $1, \dots, \text{len}(l_k^{\theta_c})$  do
6        $l_k^{\theta'}[i] \leftarrow l_k^{\theta'}[i] + l_k^{\theta_c}[i] \times |d_c|$ 
7        $L_w[i] \leftarrow L_w[i] + |d_c|$ 
8     end
9   end
10  for  $j$  in  $1, \dots, \text{len}(l_k^{\theta'})$  do
11    if  $L_w[j] > 0$  then
12       $l_k^{\theta'}[j] \leftarrow \frac{l_k^{\theta'}[j]}{L_w[j]}$ 
13    else
14       $l_k^{\theta'}[j] \leftarrow l_k^\theta[j]$ 
15    end
16  end
17 end
18 return  $\theta'$ 

```

4 Performance Evaluation

To evaluate the performance of AdaptiveFL, we implemented it using PyTorch. For a fair comparison, we adopted the same SGD optimizer with a learning rate of 0.01 and a momentum of 0.5 for all the investigated FL methods. For local training, we set the batch size to 50 and the local epoch to 5. All the experiments were conducted on a Ubuntu workstation with one Intel i9 13900k CPU, 64GB memory, and one NVIDIA RTX 4090 GPU.

4.1 Experimental Settings

Data Settings. We conducted experiments on three well-known datasets, i.e., CIFAR-10, CIFAR-100 [15], and FEMNIST [16]. For both CIFAR-10 and CIFAR-100, we assumed that there were 100 clients participating in FL. For FEMNIST, there were 180 clients involved. In each round, 10% of the clients will be selected for local training. We considered both IID and non-IID scenarios for CIFAR-10 and CIFAR-100, where we adopted the Dirichlet distribution to control the data heterogeneity. Here, the smaller the coefficient α , the higher the heterogeneity of the data. Note that FEMNIST is naturally non-IID distributed.

Table 1. Split settings for VGG16 ($p = 3$).

VGG16 Level	Pruning Configuration		Model Size		
	r_w	I	#PARAMS	#FLOPS	ratio
L_1	1.00	N/A	33.65M	333.22M	1.00
M_1	0.66	8	16.81M	272.17M	0.50
M_2		6	15.41M	239.95M	0.46
M_3		4	14.84M	203.41M	0.44
S_1	0.40	8	8.39M	239.00M	0.25
S_2		6	6.48M	191.31M	0.19
S_3		4	5.67M	139.07M	0.17

Device Heterogeneity Settings. To simulate the heterogeneity of devices, we set up three types of clients (i.e., weak, medium, and strong clients) and three levels of models (i.e., small, medium, and large models), where weak devices can only accommodate weak models, medium devices can train medium or small models, while strong devices can accommodate models of any type. For the following experiments, we set the proportion of weak, medium, and strong devices to 4: 3: 3 by default. To show the generality of our AdaptiveFL framework, we conducted experiments based on two widely used models (i.e., VGG16 [17] and ResNet18 [18]), where Table 1 shows the split settings of VGG16.

4.2 Performance Comparison

We compared AdaptiveFL with four baseline methods, i.e., All-Large [1], Decoupled [1], HeteroFL [5], and ScaleFL [7]. For All-Large, we trained the L_1 model with all clients under the classic FedAvg [1]. For Decoupled, we trained separate models (i.e., L_1 , M_1 , S_1 models) for each level using the available data of affordable clients. For HeteroFL and ScaleFL, we created their corresponding submodels at different levels. Table 2 shows the comparison results, where the notations “avg” and “full” denote the average accuracy of submodels at different levels (i.e., L_1 , M_1 , S_1) and the accuracy of the global model, respectively.

Global Model Performance. From Table 2, we can find that Decoupled has the worst inference performance in all the cases, since its submodels are only aggregated with the models at the same levels. However, AdaptiveFL can achieve up to 2.95% and 3.12% better inference than the second-best methods for ResNet18 and VGG16, respectively. Note that AdaptiveFL can achieve better results compared with All-Large, indicating that AdaptiveFL can improve the FL performance in non-resource scenarios.

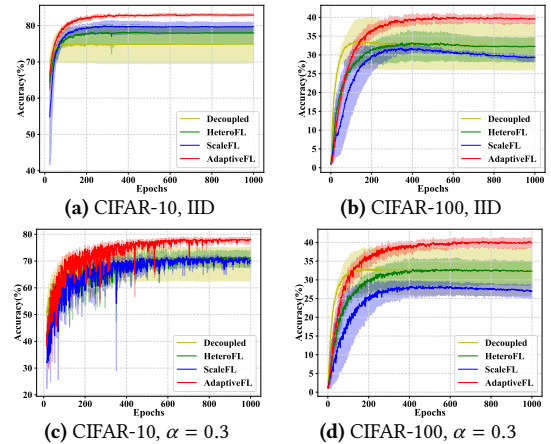


Figure 2. Learning curves of AdaptiveFL and three baselines.

Submodel Performance. Figure 2 shows the learning trends of all methods on CIFAR-10/100 based on VGG16, where solid lines represent the “avg” accuracy of submodels. We can find that AdaptiveFL can achieve the best inference performance with the least variations for both non-IID and IID scenarios. For different heterogeneous FL methods, Figure 3 presents the shapes of VGG16 submodels together with their test accuracy information. We can find that AdaptiveFL consistently outperforms other heterogeneous FL methods under the premise of satisfying the resource constraints,

Table 2. Test accuracy (%) comparison of avg/full models (the best and second-best results are in **bold** and underlined, respectively).

Model	Algorithm	CIFAR-10						CIFAR-100						FEMNIST	
		IID		$\alpha = 0.6$		$\alpha = 0.3$		IID		$\alpha = 0.6$		$\alpha = 0.3$		-	
		avg	full	avg	full	avg	full	avg	full	avg	full	avg	full	avg	full
VGG16	All-Large [1]	-	79.76	-	77.29	-	74.95	-	40.71	-	41.13	-	40.34	-	85.21
	Decoupled [1]	75.02	69.80	72.95	67.58	69.11	62.91	33.66	26.67	33.37	26.53	32.86	26.54	78.45	70.13
	HeteroFL [5]	77.98	74.96	75.18	72.69	71.18	67.59	32.22	28.13	32.92	28.82	32.32	28.68	77.69	71.75
	ScaleFL [7]	79.94	78.12	76.08	75.07	71.71	70.42	31.86	32.17	30.82	30.57	28.36	29.61	71.58	67.36
	AdaptiveFL	82.97	83.14	81.12	81.31	78.85	78.99	40.61	40.93	37.87	38.88	40.95	41.17	87.38	88.13
ResNet18	All-Large [1]	-	68.37	-	67.03	-	64.28	-	35.08	-	34.74	-	33.84	-	83.94
	Decoupled [1]	63.23	55.56	59.21	52.59	55.82	49.65	24.58	22.35	25.22	20.14	24.06	20.02	74.37	65.20
	HeteroFL [5]	70.44	65.37	65.97	60.33	60.32	55.83	30.43	27.74	30.23	23.59	28.96	23.04	77.50	69.35
	ScaleFL [7]	76.34	76.51	72.68	72.91	67.26	67.50	40.30	40.46	38.91	37.86	36.82	36.56	83.64	83.79
	AdaptiveFL	77.14	77.20	74.72	74.89	70.61	70.97	41.09	41.15	39.14	39.56	39.15	39.65	87.11	87.30

which indicates the effectiveness of our fine-grained width-wise model pruning mechanism. Interestingly, we can find that 1.0× large models of HeteroFL and ScaleFL perform worse instead their 0.25× small counterparts. Conversely, as the model size increases, AdaptiveFL can achieve better results, indicating that it can smoothly transfer the knowledge learned by the submodels into large models.

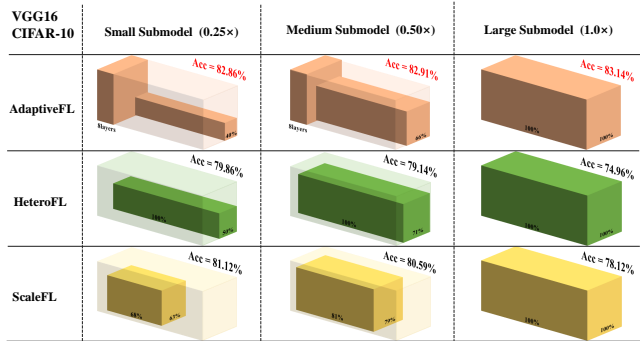


Figure 3. Comparison of submodels at different levels.

4.3 Impacts of Different Configurations

Numbers of Participating Clients. To evaluate the scalability of AdaptiveFL, we conducted experiments considering different numbers of participating clients, i.e., $K = 50, 100, 200,$ and 500 , respectively, on CIFAR-10 using ResNet18. Figure 4 compares AdaptiveFL with three baselines within a non-IID scenario ($\alpha = 0.6$), where AdaptiveFL can always achieve the highest accuracy.

Proportions of Different Devices. Table 3 shows the performance of AdaptiveFL with different proportions (i.e., 8:1:1, 1:8:1, 1:1:8, and 4:3:3) of weak, medium, and strong devices on CIFAR-10. We can find that AdaptiveFL can achieve the best test accuracy in all cases. Note that as the proportion of strong devices increases, the global model performance of all FL methods improves.

Table 3. Performance comparison (%) under different proportions.

Algorithm	Proportion							
	4:3:3		8:1:1		1:8:1		1:1:8	
	avg	full	avg	full	avg	full	avg	full
All-Large	-	79.76	-	79.76	-	79.76	-	79.76
HeteroFL	77.98	74.96	72.43	64.44	75.94	65.96	81.26	81.12
ScaleFL	79.94	78.12	75.89	72.03	78.40	72.30	82.55	82.81
AdaptiveFL	82.95	83.14	81.62	81.93	82.78	82.89	82.82	83.24

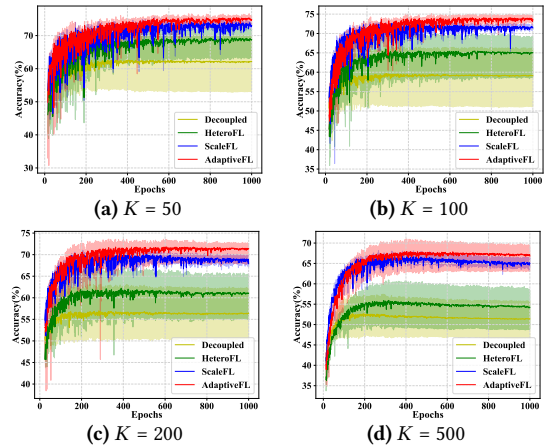


Figure 4. Learning curves on different numbers of involved devices.

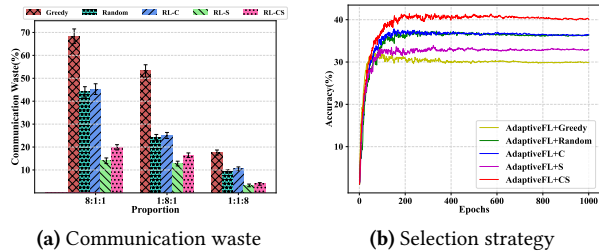
4.4 Ablation Study

Ablation of Fine-grained Pruning. To evaluate both fine- and coarse-grained pruning, we set p to 3 and 1 for each level, respectively. Table 4 presents the ablation results of AdaptiveFL considering the effect of our fine-grained pruning method, showing that the fine-grained pruning method can achieve up to 9.38% inference accuracy improvements for AdaptiveFL. Note that the fine-grained methods can consistently achieve better inference results than their coarse-grained counterparts, since the fine-grained ones can better transfer the knowledge of small models to large models.

Table 4. Ablation of fine-grained pruning (accuracy on “full”).

Dataset	Model	Grained	Distribution		
			IID	$\alpha = 0.6$	$\alpha = 0.3$
CIFAR-10	VGG16	coarse	80.1	78.9	74.27
		fine	83.14 (+3.04)	81.31 (+2.41)	78.99 (+4.72)
	ResNet18	coarse	72.43	71.92	66.07
		fine	77.2 (+4.77)	74.89 (+2.97)	70.97 (+4.9)
CIFAR-100	VGG16	coarse	38.91	39.43	39.29
		fine	40.93 (+2.02)	38.88 (-0.55)	41.17 (+1.88)
	ResNet18	coarse	31.77	35.52	34.73
		fine	41.15 (+9.38)	39.56 (+4.04)	39.65 (+4.92)

Ablation of RL-based Client Selection. To evaluate the effectiveness of our RL-based client selection strategy, we developed four variants of AdaptiveFL: i) “AdaptiveFL+Greedy” that always dispatches the largest model for each selected client; ii) “AdaptiveFL+Random” that selects clients for local training randomly; iii) “AdaptiveFL+C” that selects clients only based on curiosity reward; and iv) “AdaptiveFL+S” that selects clients only using resource rewards. Moreover, we use “AdaptiveFL+CS” to indicate the original AdaptiveFL implemented in Algorithm 1.



(a) Communication waste (b) Selection strategy
Figure 5. Ablation study for RL-based client selection.

Figure 5 presents the ablation study results on CIFAR-100 with ResNet18 following IID distribution. To indicate the similarity between a sending model and its corresponding receiving model, we introduce a new metric called *communication waste rate*, defined as $1 - \sum(\text{size}(ML_{back})) / \sum(\text{size}(ML_{send}))$. The lower the rate, the closer the two models are, leading to less local pruning efforts. From Figure 5, we can find that our approach can achieve the highest accuracy with low communication waste (second only to RL-S).

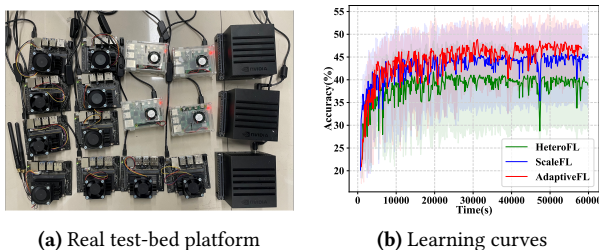
4.5 Evaluation on Real Test-bed

Based on our real test-bed platform, we conducted experiments on a non-IID IoT dataset (i.e., Widar [19]) with MobileNetV2 [20] models. We assumed that the FL-based AIoT system has 17 devices, each training round involves 10 selected devices, whose detail heterogeneous configurations are shown in Table 5.

Table 5. Real test-bed platform configuration.

Type	Device	Comp	Mem	Num
Client-Weak	Raspberry Pi 4B	ARM Cortex-A72 CPU	2G	4
Client-Medium	Jetson Nano	128-core Maxwell GPU	8G	10
Client-Strong	Jetson Xavier AGX	512-core NVIDIA GPU	32G	3
Server	Workstation	NVIDIA RTX 4090 GPU	64G	1

Figure 6 presents the AIoT devices used in our experiment and the comparison results obtained from our real test-bed platform. We can observe that AdaptiveFL achieves the best inference results even in real scenarios compared to all baselines.



(a) Real test-bed platform (b) Learning curves
Figure 6. Real test-bed experiment.

5 Conclusion

This paper presented a novel Federated Learning (FL) approach named AdaptiveFL to enable effective knowledge sharing among heterogeneous devices for large-scale Artificial Intelligence of Things (AIoT) applications, considering the varying on-the-fly hardware resources of AIoT devices. Based on our proposed fine-grained width-wise model pruning mechanism, AdaptiveFL supports the generation of different local models, which will be selectively dispatched to their AIoT device counterparts in an adaptive manner according to their available local training resources. Experimental results show that our approach can achieve better inference performance than state-of-the-art heterogeneous FL methods.

Acknowledgment

This research is supported by the Natural Science Foundation of China (62272170), “Digital Silk Road” Shanghai International Joint Lab of Trustworthy Intelligent Software (22510750100), and the National Research Foundation Singapore and DSO National Laboratories under the AI Singapore Programme (AISG Award No: AISG2-RP-2020-019). Ming Hu and Mingsong Chen are the corresponding authors.

References

- [1] Brendan McMahan, Eider Moore, Daniel Ramage, Seth Hampson, and Blaise Agüera y Arcas. Communication-efficient learning of deep networks from decentralized data. In *Proceedings of Artificial intelligence and statistics*, pages 1273–1282, 2017.
- [2] Ming Hu, E Cao, Hongbing Huang, Min Zhang, Xiaohong Chen, and Mingsong Chen. Aiotml: A unified modeling language for aiot-based cyber-physical systems. *IEEE Transactions on Computer-Aided Design of Integrated Circuits and Systems*, 42(11):3545–3558, 2023.
- [3] Xinqian Zhang, Ming Hu, Jun Xia, Tongquan Wei, Mingsong Chen, and Shiyun Hu. Efficient federated learning for cloud-based aiot applications. *IEEE Transactions on Computer-Aided Design of Integrated Circuits and Systems*, 40(11):2211–2223, 2021.
- [4] Ming Hu, Zeke Xia, Dengke Yan, Zhihao Yue, Jun Xia, Yihao Huang, Yang Liu, and Mingsong Chen. Gitfl: Uncertainty-aware real-time asynchronous federated learning using version control. In *IEEE Real-Time Systems Symposium (RTSS)*, pages 145–157, 2023.
- [5] Enmao Diao, Jie Ding, and Vahid Tarokh. Heterofl: Computation and communication efficient federated learning for heterogeneous clients. *arXiv*, 2020.
- [6] Minjae Kim, Sangyoon Yu, Suhyun Kim, and Soo-Mook Moon. Depthfl: Depth-wise federated learning for heterogeneous clients. In *Proceedings of International Conference on Learning Representations*, 2022.
- [7] Fatih Ilhan, Gong Su, and Ling Liu. Scalefl: Resource-adaptive federated learning with heterogeneous clients. In *Proceedings of the IEEE/CVF Conference on Computer Vision and Pattern Recognition*, pages 24532–24541, 2023.
- [8] Yae Jee Cho, Andre Manoel, Gauri Joshi, Robert Sim, and Dimitrios Dimitriadis. Heterogeneous ensemble knowledge transfer for training large models in federated learning. In *Proceedings of International Joint Conference on Artificial Intelligence*, 2022.
- [9] Tao Lin, Lingjing Kong, Sebastian U Stich, and Martin Jaggi. Ensemble distillation for robust model fusion in federated learning. *Advances in Neural Information Processing Systems*, 33:2351–2363, 2020.
- [10] Ming Hu, Wenxue Duan, Min Zhang, Tongquan Wei, and Mingsong Chen. Quantitative timing analysis for cyber-physical systems using uncertainty-aware scenario-based specifications. *IEEE Transactions on Computer-Aided Design of Integrated Circuits and Systems*, 39(11):4006–4017, 2020.
- [11] Hao Li, Asim Kadav, Igor Durdanovic, Hanan Samet, and Hans Peter Graf. Pruning filters for efficient convnets. In *Proceedings of ICLR*, 2016.
- [12] Ming Hu, Jiepin Ding, Min Zhang, Frédéric Mallet, and Mingsong Chen. Enumeration and deduction driven co-synthesis of ccs1 specifications using reinforcement learning. In *2021 IEEE Real-Time Systems Symposium (RTSS)*, pages 227–239, 2021.
- [13] Ming Hu, Min Zhang, Frédéric Mallet, Xin Fu, and Mingsong Chen. Accelerating reinforcement learning-based ccs1 specification synthesis using curiosity-driven exploration. *IEEE Transactions on Computers*, 72(5):1431–1446, 2023.
- [14] Marc Bellemare, Sriram Srinivasan, Georg Ostrovski, Tom Schaul, David Saxton, and Remi Munos. Unifying count-based exploration and intrinsic motivation. *Advances in neural information processing systems*, 29, 2016.
- [15] Alex Krizhevsky, Geoffrey Hinton, et al. Learning multiple layers of features from tiny images. 2009.
- [16] Sebastian Caldas, Peter Wu, Tian Li, Jakub Konečný, H. Brendan McMahan, Virginia Smith, and Ameet Talwalkar. LEAF: A benchmark for federated settings. *CoRR*, abs/1812.01097, 2018.
- [17] Karen Simonyan and Andrew Zisserman. Very deep convolutional networks for large-scale image recognition. *arXiv preprint arXiv:1409.1556*, 2014.
- [18] Kaiming He, Xiangyu Zhang, Shaoqing Ren, and Jian Sun. Deep residual learning for image recognition. In *Proceedings of the IEEE/CVF Conference on Computer Vision and Pattern Recognition*, pages 770–778, 2016.
- [19] Samiul Alam, Tuo Zhang, Tiantian Feng, Hui Shen, Zhichao Cao, Dong Zhao, JeongGil Ko, Kiran Somasundaram, Shrikanth S Narayanan, Salman Avestimehr, et al. Fedaiot: A federated learning benchmark for artificial intelligence of things. *arXiv*, 2023.
- [20] Mark Sandler, Andrew Howard, Menglong Zhu, Andrey Zhmoginov, and Liang-Chieh Chen. Mobilenetv2: Inverted residuals and linear bottlenecks. In *Proceedings of the IEEE/CVF Conference on Computer Vision and Pattern Recognition*, pages 4510–4520, 2018.